Materials Science & Engineering A 733 (2018) 1–8

Contents lists available at ScienceDirect

Materials Science & Engineering A

journal homepage: www.elsevier.com/locate/msea

Effect of holding time at an intercritical temperature on the microstructure and tensile properties of a ferrite-martensite dual phase steel

M. Balbi*, I. Alvarez-Armas, A. Armas

Instituto de Física Rosario, National University of Rosario, Bv. 27 de Febrero 210 bis, 2000 Rosario, Santa Fe, Argentina

ARTICLE INFO

Keywords:
Dual phase steels
Intercritical heat treatments
Partitioning
Microstructure
Mechanical properties

ABSTRACT

To analyze the influence of the initial microstructure in the production of a dual phase (DP) steel on the mechanical properties, a commercial DP steel was subjected to two heat treatments (HT): step quenching (SQ) and intermediate quenching (IQ). SQ samples were austenitized at 930 °C for 20 min, then annealed at 830 °C for 5, 15, 30, 60 and 120 min and finally water quenched. Shorter annealing times show allotriomorphic ferrite and martensite while at longer time polygonal ferrite is formed. Tensile tests showed that yield and tensile strength are higher than those of the commercial DP steel and besides, the uniform elongation is smaller. IQ samples were water quenched after austenitization and then annealed at 830 °C for the same holding times and water quenched again. The microstructure consists of martensite dispersed in a ferrite matrix. The remarkable results are that these samples had similar tensile properties to that of the as-received DP steel. Tensile properties were analyzed as a function of the characteristic microstructure and the assessment of the alloying elements partition during the different HTs. Evaluation of the Kolmogorov-Johnson-Mehl-Avrami theory indicates that the transformation in SQ and in IQ samples corresponds to a diffusional process.

1. Introduction

Dual-phase (DP) steels offer an outstanding combination of high strength and good ductility as a result of their microstructure, in which a hard martensitic phase is dispersed in a soft ferrite matrix. They are commonly used in industries, specially the automobile industry. Automobile components of DP steels include car body panels, wheels, bumpers [1,2], etc. in which the current drive is to reduce weight (for improved fuel efficiency) and to achieve higher crash resistance [3] (making them safer for consumers).

Intercritical heat treatment is the simplest way to produce dual phase microstructure from low-alloyed steels. Before heat treatment at the ($\alpha + \gamma$) region, the initial microstructure can be martensite, ferrite + pearlite or austenite, which will affect the final morphologies and properties of the resultant dual microstructure obtained after quenching.

Tensile properties, formability and many other mechanical properties have been extensively studied as a function of microstructural factors such as phase volume fraction [4–6], morphology [6,7], grain size [8,9], and the corresponding deformation/strain hardening mechanisms [10,11]. Despite the extensive number of research articles published on the monotonic deformation behavior of DP steels, only a few investigators [12,13] have discussed the influence of different holding times at the intercritical temperature range on the mechanical properties of the steel.

The aim of the present investigation is to study the influence of the holding time duration at the intercritical region on the microstructural changes and on the mechanical properties of monotonic tensile test of two DP steels obtained using two simple heat treatment processes.

2. Experimental procedure

2.1. Material and heat treatments

The steel used in this investigation is a commercial dual phase steel provided in the form of a 5.3 mm thick sheet. The chemical composition in weight percent is: 0,09% C, 1,5% Mn and 0,25% Si. Before performing the intercritical heat treatments, the limits of this range of temperatures were determined with thermal expansion technique, resulting Ac1 = 740 °C and Ac3 = 880 °C using a heating rate of 1 °C/s. As a reference point, the transformation temperatures of the intercritical region, Ac1 and Ac3, were also calculated according to the equation derived by Andrews [14], which depends on the chemical composition. These temperatures are: Ac1 = 720 °C and Ac3 = 860 °C. According to these results, the austenitization temperature was taken at 930 °C and the temperature within the intercritical region was fixed at

* Corresponding author.
E-mail address: balbi@ifir-conicet.gov.ar (M. Balbi).

https://doi.org/10.1016/j.msea.2018.07.029
Received 20 February 2018; Received in revised form 6 July 2018; Accepted 9 July 2018
Available online 11 July 2018
0921-5093/

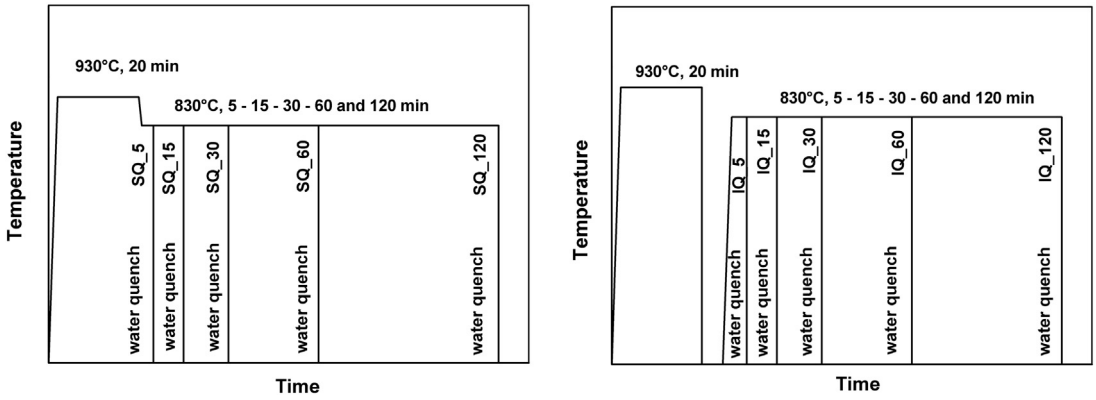

Fig. 1. Heat treatments of the production routes.

830 °C.

Fig. 1 shows two different production routes to produce the ferritic-martensitic structure from the as-received steel. The first one (Fig. 1**a**) consisted in austenitizing the steel at 930 °C during 20 min, then annealed at 830 °C in the intercritical range of temperatures for 5, 15, 30, 60 and 120 min and finally water quenched. These specimens will be called as: SQ_5, SQ_15, SQ_30, SQ_60 and SQ_120. In the second process (Fig. 1**b**), samples were austenitezed at 930 °C during 20 min and water quenched to produce a fully martensite phase. Then, these specimens were re-heated up to 830 °C for 5, 15, 30, 60, and 120 min and water quenched again. These specimens will be referred as: IQ_5, IQ_15, IQ_30, IQ_60 and IQ_120.

2.2. Microstructural evaluation

Scanning Electron Microscopy (SEM) samples were prepared using standard metallographic grinding and polishing techniques and finally etched firstly with 3% nital and then with 4% picral (4 g picric acid in 100 ml ethyl alcohol). Phase volume fractions were determined using the point counting method following ASTM E 562-02 norm [15] and using the image J software. Energy Dispersive X-ray Spectroscopy (EDS) detector mounted on the SEM was used to analyze the elements distribution in both ferrite and martensite phases.

Electron Backscattered Diffraction (EBSD) techniques were carried out on selected specimens to further examine the microstructure that occurs during the different heat treatments.

EBSD samples were prepared by standard mechanical grinding and polishing procedures, finishing with colloidal silica. EBSD analysis were conducted in a high-resolution scanning electron microscope (SEM) equipped with a Field Emission Gun (FEG). Data was recorded and analyzed using the EDAX-TSL OIM Analysis software package.

X-ray diffractograms analysis was applied to estimate the lattice parameter of the martensite according to its carbon content. They were performed using Cu Kα radiation in a Philiphs X′ Pert pro MDP goniometer.

2.3. Tensile specimens

Tensile test were performed in an Instron 3382 machine at room temperature. The specimens were prepared according to ASTM E8M norm [16] using an electro discharge machine (EDM). The main dimensions of the specimens were 100 mm length and 10 mm width.

3. Results

3.1. Microstructures

Fig. 2 shows a SEM image of the as-received DP steel. It consists of 20% martensite phase embedded in a ferrite matrix. Hereafter, the microstructures obtained from the different heat treatments are described in separate sections.

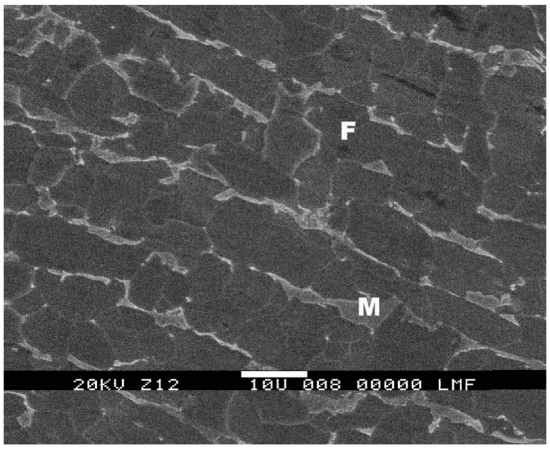

Fig. 2. SEM image of the as-received DP material.

3.1.1. Step quenching heat treatments

The SQ heat treatments were performed using two furnaces in simultaneous, one at 930 °C and the other at 830 °C. Samples were placed in the first furnace during 20 min and then rapidly changed to the second one during different holding times: 5, 15, 30, 60 and 120 min and then quenched in water. During the intercritical annealing, part of the austenite was isothermally transformed into ferrite, obtaining at 830 °C a mixture of two phases ferrite and austenite. The subsequent quenching transforms the austenite into lath martensite, obtaining the dual ferrite-martensite microstructure as the final product. Fig. 3 shows SEM micrographs for the different holding times at the intercritical temperature.

According to the ISIJ Bainite Committee Notation two different morphologies of ferrite can occur during the transformation in the intercritical range of temperatures: grain boundary allotriomorphs and polygonal ferrite [17].

Fig. 3**a** shows the microstructure of the sample treated for 5 min at 830 °C (SQ_5) and then water quenched; it consists practically of fully lath martensite structure and just few ferrite grains. In SQ_15 sample, martensite and allotriomorphic ferrite as well as a very small amount of polygonal ferrite are present. As the holding time at 830 °C increases (SQ_30 and SQ_60), the amount of ferrite grains increases as either polygonal ferrite or allotriomorphic ferrite. These results can be seen in Fig. 3**d**, in which the amount of polygonal ferrite prevails and only few grains of allotriomorphic ferrite are observed. The microstructure of the SQ_120 sample is characterized by large and equiaxed grain structure, which consists of polygonal ferrite and martensite (Fig. 3**e**).

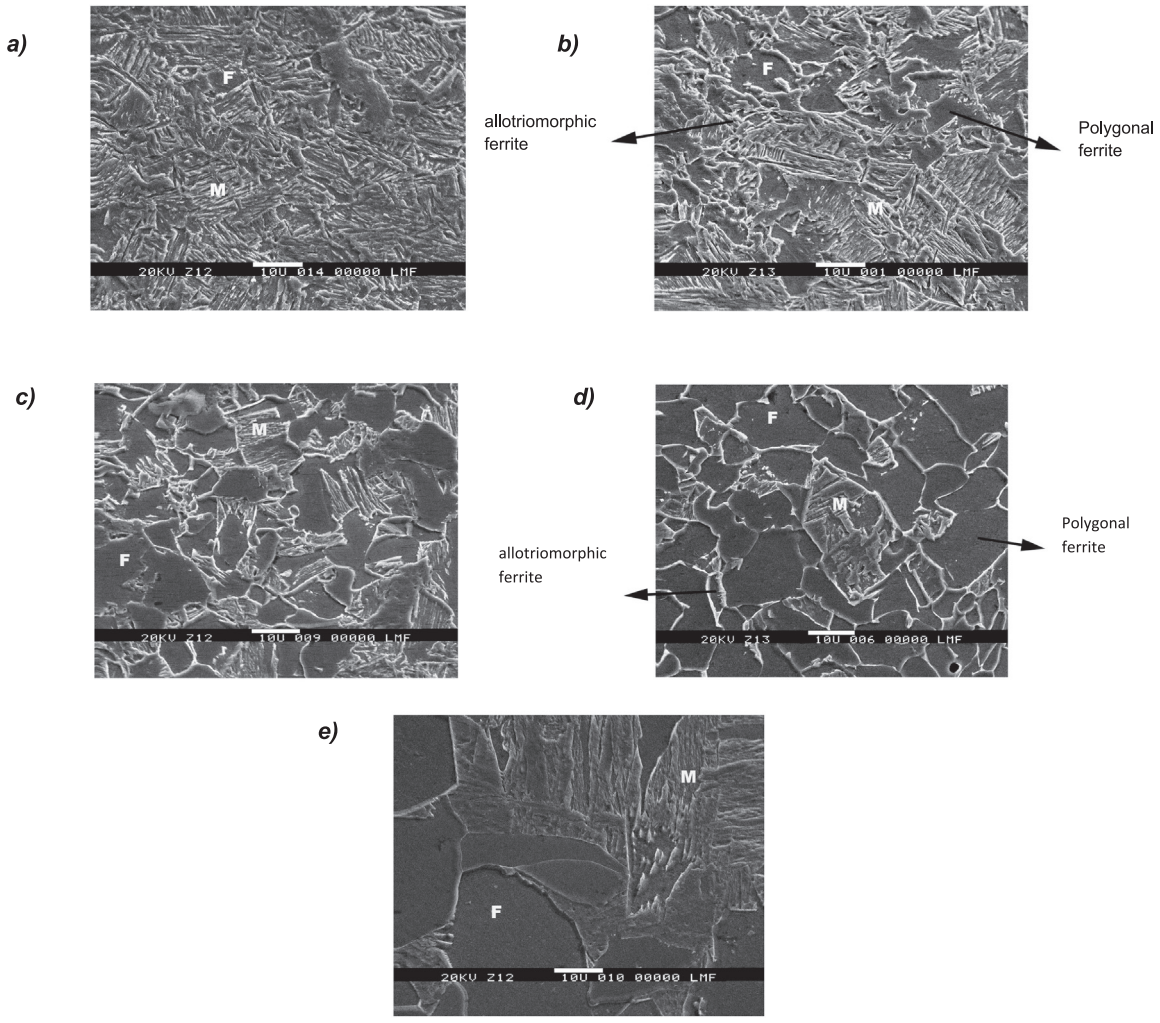

Fig. 3. SEM images of (a) SQ_5, (b) SQ_15, (c) SQ_30, (d) SQ_60 and (e) SQ_120 samples.

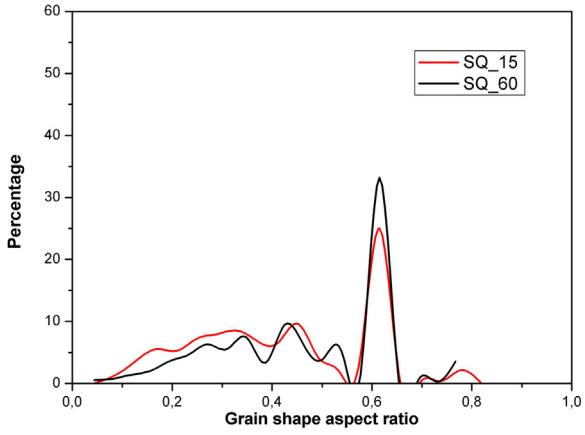

Fig. 4. Representation of the grain shape aspect ratio of SQ_15 and SQ_60 samples.

Fig. 4 shows the EBSD analysis of the grain shape aspect ratio of the grains in samples SQ_15 and SQ_60. Ratio 1 corresponds to perfectly equiaxed grains, while towards zero the grains are completely elongated. Accordingly, the grains in SQ_15 are less equiaxed than in the SQ_60; this fact can be rationalized as a result of hold time duration in the intercritical temperature range where the ferritic grains are mostly allotriomorphics and follow the shape of the austenite grain boundaries.

3.1.2. Intermediate quenching heat treatments

When the as-received material is heated in the first furnace at 930 °C, the ferritic-martensitic structure of the DP steel is completely austenitized. The subsequent quenching produces fully lath martensite structure, with the c/a relation close to unity (c/a = 1.0037 data obtained by X-ray analysis) because of the low amount of carbon. Then, the samples were placed in a second furnace heated at 830 °C and hold for 5, 15, 30, 60 and 120 min before water quenching. At this temperature, because of energy reasons, the steel easily transform from BCT to BCC structure while the austenite starts to grow at numerous sites provided by the prior austenite grain boundaries and martensite lath boundaries. After quenching, the austenite transforms into the so-called fibrous martensite [7,18,19] and ferrite.

Fig. 5**a** shows a SEM micrograph of the IQ_ 5 sample that consists practically of ferrite grains with a very small amount of martensite. As the holding time increases, austenite grains grow, and consequently after quenching the amount of martensite is higher. It is interesting to note that the fine fibrous structure of the martensite is observed in almost all the samples except in IQ_120 where it is less defined. As well, more equiaxed grain structure can be observed at IQ_60 and at IQ_120. In order to evaluate the increased trend towards more equiaxed grains with holding time, the grain-shape aspect ratio of the structure was assessed by EBSD analysis. For this purpose, the IQ_15 and IQ_60 samples (Fig. 6) were analyzed. The graph clearly gives evidence of this

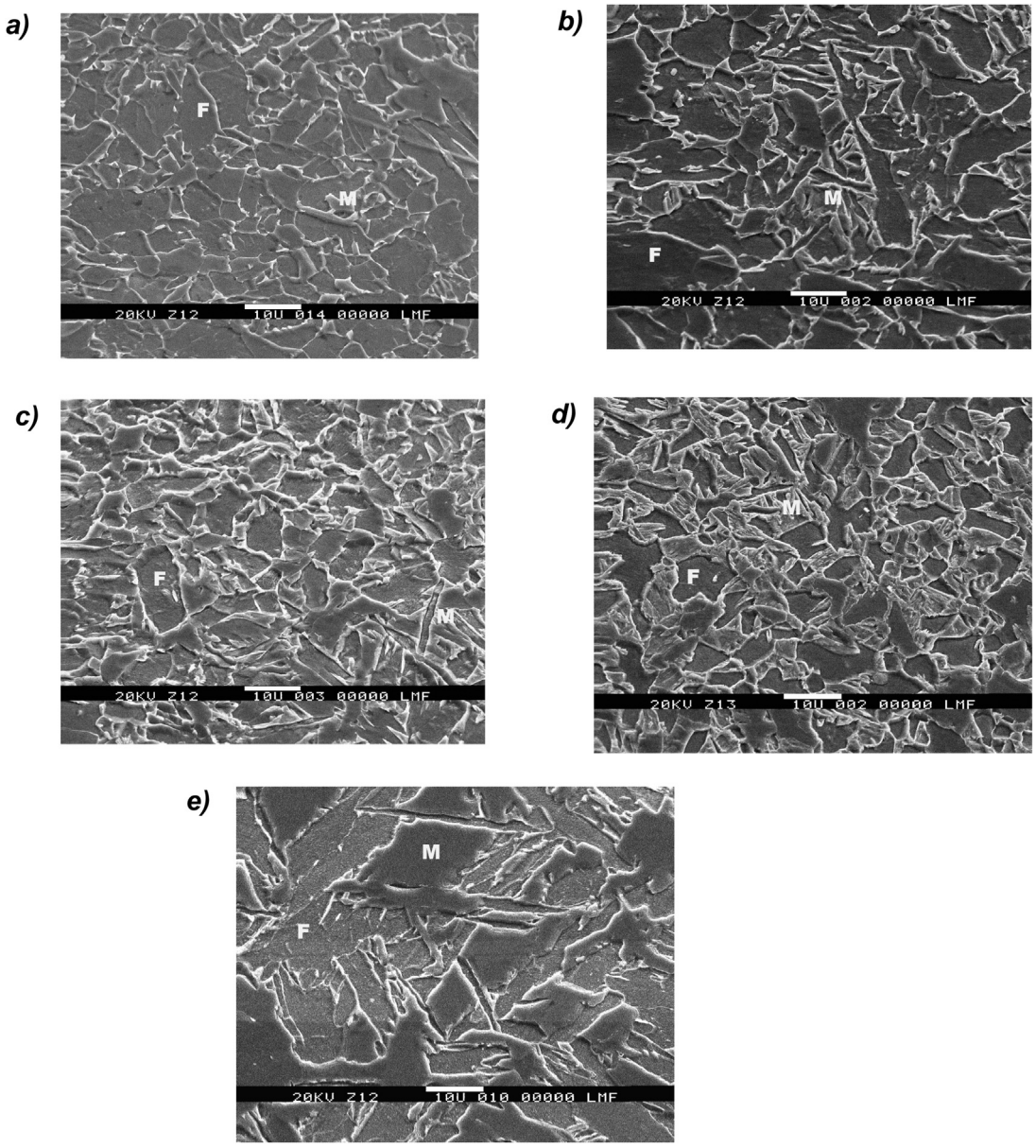

Fig. 5. SEM images of (a) IQ_5, (b) IQ_15, (c) IQ_30, (d) IQ_60 and (e) IQ_120 samples.

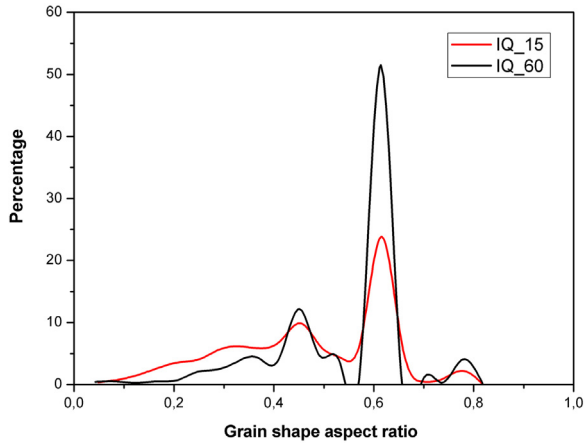

Fig. 6. Representation of grain shape aspect ratio of IQ-15 and IQ_60 samples.

remarkable increase in the frequency distribution of aspect ratio at 0.6 for IQ_60.

3.2. Tensile tests

Uniaxial tensile behavior of SQ and IQ specimens tested at room temperature are shown in Fig. 7. In addition, Table 1 summarizes the main tensile properties such as yield and tensile strength and elongation, as well as the phase proportion of ferrite and martensite for each heat treatment.

In Fig. 7 is interesting to note that regardless of the heat treatment, either SQ or IQ, the tensile behavior of each group of samples are very similar and additionally is remarkable that the IQ and the as-received samples present very similar tensile behavior. Table 1 clearly shows the similarities and differences between both groups of samples. For the IQ samples, yield strength ranges between 360 and 400 MPa, tensile strength between 610 and 670 MPa, total elongation between 44% and 47% and uniform elongation around 17–22%. A completely different result is observed in SQ samples, where although yield and tensile

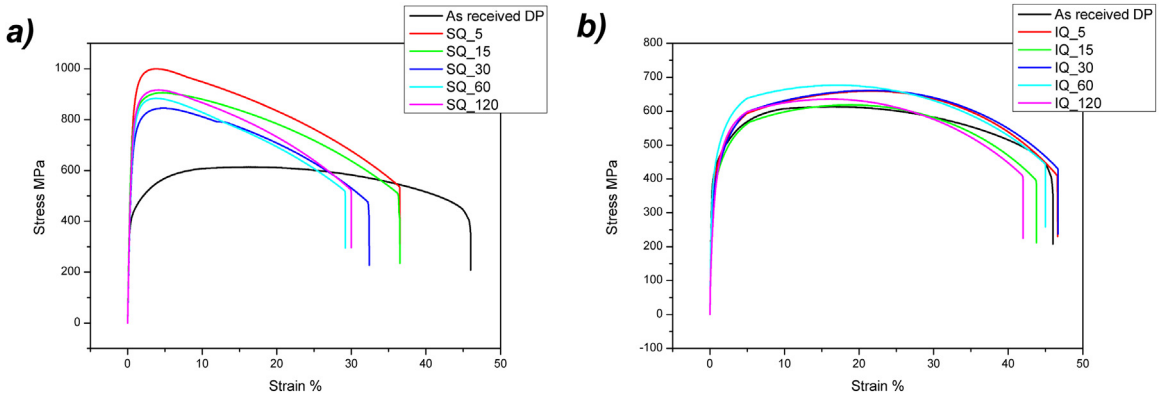

Fig. 7. Engineering stress-strain curves of (a) SQ and (b) IQ samples.

Table 1
Tensile properties and phase proportions for the SQ and IQ samples, as well as the as-received commercial DP steel.

	σ_Y [MPa]	σ_{TS} [MPa]	Uniform Elongation [%]	Total Elongation [%]	Proportion of phases
DP_as-received	430	610	14	45	80%F—20%M
IQ_5	370	660	22	46,6	85%F—15%M
IQ_15	360	610	18	43,8	70%F—30%M
IQ_30	380	660	21,5	46,7	60%F—40%M
IQ_60	400	670	17	45	50%F—50%M
IQ_120	370	640	15	42	50%F—50%M
SQ_5	810	1000	3,7	36,5	15%F—85%M
SQ_15	730	900	4	36,5	35%F—65%M
SQ_30	670	850	4,5	32,4	40%F—60%M
SQ_60	730	890	3,8	29	50%F—50%M
SQ_120	730	900	3,5	30	55%F—45%M

strength are higher (they almost double their values) than those of the commercial DP steel, the uniform elongation is very small and can reach values around 3–4%. Consequently, due mainly to the lack of suitable elongation, the step quenching heat treatment seems not to be beneficial for commercial purpose.

4. Discussions

The DP microstructure contains hard martensitic islands embedded in a generally continuous soft ferrite. When these steels deform, the strain is concentrated in the lower-strength ferrite; moreover, this plastic deformation spread into the ferrite limited by the neighboring grains of martensite, resulting in an accumulation of stress concentration in the ferrite-martensite interface. In general, it was found that yield strength and tensile strength are increased due to grain refinement, and it is accompanied by a deterioration of ductility. However it was shown that this is not applied to DP steels. In DP steels the refinement of martensite island or the distribution of fibrous martensite enhance the ductility of the steel [20]. Fig. 8 shows optical images and the result of applying the image J software in samples SQ_60 and IQ_60, in which the size effect of martensite particles define the tensile properties of the microstructure. As can be seen, both samples have similar phase proportions but the size of the martensite phase for sample IQ_60 is smaller than that of SQ_60. This could be also observed in SEM images Figs. 3 and 5.

Concerning Table 1 and Fig. 7, it is interesting to analyze these results. They show that regardless of the holding time applied to the IQ and SQ specimen group, phase proportion seems not to play an essential role in their tensile properties. Indeed, yield and tensile strength as well as total elongation do not vary significantly with the variation of phase proportion. Alternatively, it is known that alloying elements are a very important point in the determination of the microstructure in Fe-C alloys. Analysis of the main alloying elements by EDS indicates that the partition of them between ferrite and martensite is the same in both SQ and IQ samples except for manganese (Mn). Fig. 9 shows a remarkable variation in the partition of Mn in the IQ samples but not in the SQ samples.

As it is well-known, Mn has higher solubility in austenite than in ferrite [21,22] and notably the diffusion coefficients are comparatively lower in austenite than in ferrite [23]. As was aforementioned, SQ samples are produced first austenitizing the as-received DP steel during a period of time and then heated at the intercritical temperature for different holding times. Consequently, the growth of ferrite in the intercritical range of temperatures is attained more for the diffusion of C than for Mn atoms. Therefore, the Mn partition between phases does not change during the microstructure formation. That means that Mn atoms can remain in solid solution in both phases strengthening the matrix. On the contrary, IQ samples start in the intercritical region from a martensitic structure rich in Mn atoms in solid solution after quenching from the austenite region. In the region the BCT martensite transforms into BCC ferrite while the austenite starts to grow at boundaries not only due to the diffusion of C but also due to the higher mobility of Mn in ferrite [23]. Thus, after quenching an appreciable difference in weight percent of Mn can be expected between ferrite and martensite phases.

In balance, the partition of Mn between the parent and growing phases during heat treatment in the intercritical region depend on the initial crystal structure - either austenite or martensite. In SQ samples, the ferrite is no more as soft and ductile as in commercial DP steel producing as a result a reduction of the ability to accumulate plastic deformation.

In order to predict the transformed volume fraction at the intercritical temperature, from austenite to ferrite in the SQ samples or from ferrite to austenite in the IQ samples, the Kolmogorov-Johnson-Mehl-Avrami theory (JMAK model) was evaluated. JMAK model describes how materials are transformed from one phase to another at a constant temperature by the process of diffusion that involves the processes of nucleation and growth [24]. According to this model, the transformed

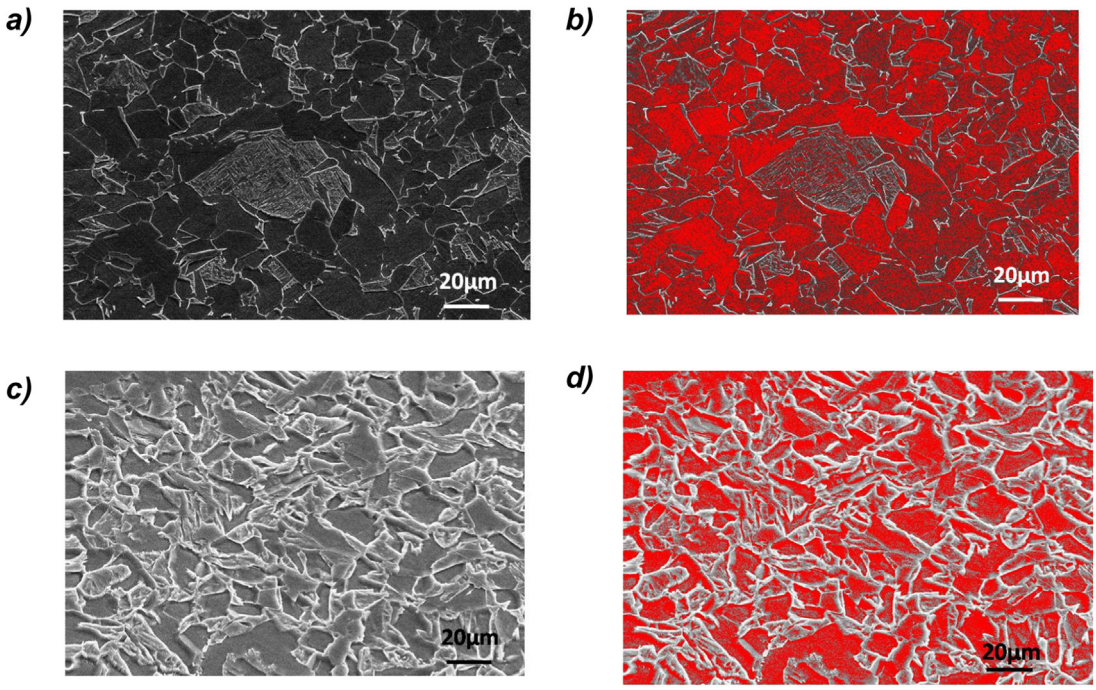

Fig. 8. (a) SQ_60 optical image, (b) SQ_60 image J software, (c) IQ_60 optical image and (d) IQ_60 image J software.

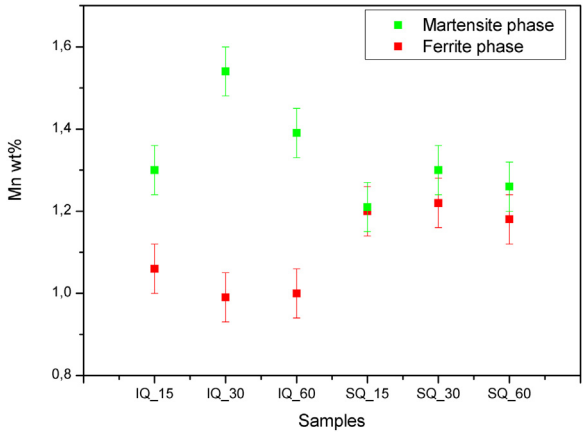

Fig. 9. Manganese partition between ferrite and martensite in IQ and SQ samples.

volume fraction (X) is determined using the following equation:

$$X = 1-\exp(-kt^n) \quad (1)$$

where t is the time in second, n the Avrami's exponent and k a constant that depends on temperature.

According to this model, when the time t tends to infinity, the fraction of transformed volume tends to unity. However, in a real transformation when the time is too long, X would tend to the equilibrium value and not to 1. According to this, X is taken as the ratio between the transformed volume fraction (V_α) at a given time and the volume fraction in equilibrium (V_e) for a specific temperature. It would be expressed as follows:

$$X = \frac{V_\alpha}{V_e} = 1-\exp(-kt^n) \quad (2)$$

Assuming that after quenching all the remaining austenite is transformed into martensite, it can be considered that the fraction of martensite after quenching is equal to the fraction of austenite at the intercritical temperature. Additionally, three more samples were added

Table 2
Phase proportions of: (a) SQ samples and (b) IQ samples.

		% Ferrite	% Martensite
a)	**SQ_0.5 (30 s)**	5	95
	SQ_5 (300 s)	15	90
	SQ_15 (900 s)	35	65
	SQ_30 (1800s)	40	60
	SQ_60 (3600 s)	50	50
	SQ_120 (7200 s)	55	45
	SQ_240 (14,400 s)	55	45
		% Ferrite	**% Martensite**
b)	**IQ_0.5 (30 s)**	94	6
	IQ_5 (300 s)	85	15
	IQ_15 (900 s)	70	30
	IQ_30 (1800s)	60	40
	IQ_60 (3600 s)	50	50
	IQ_120 (7200 s)	50	50
	IQ_240 (14400 s)	50	50

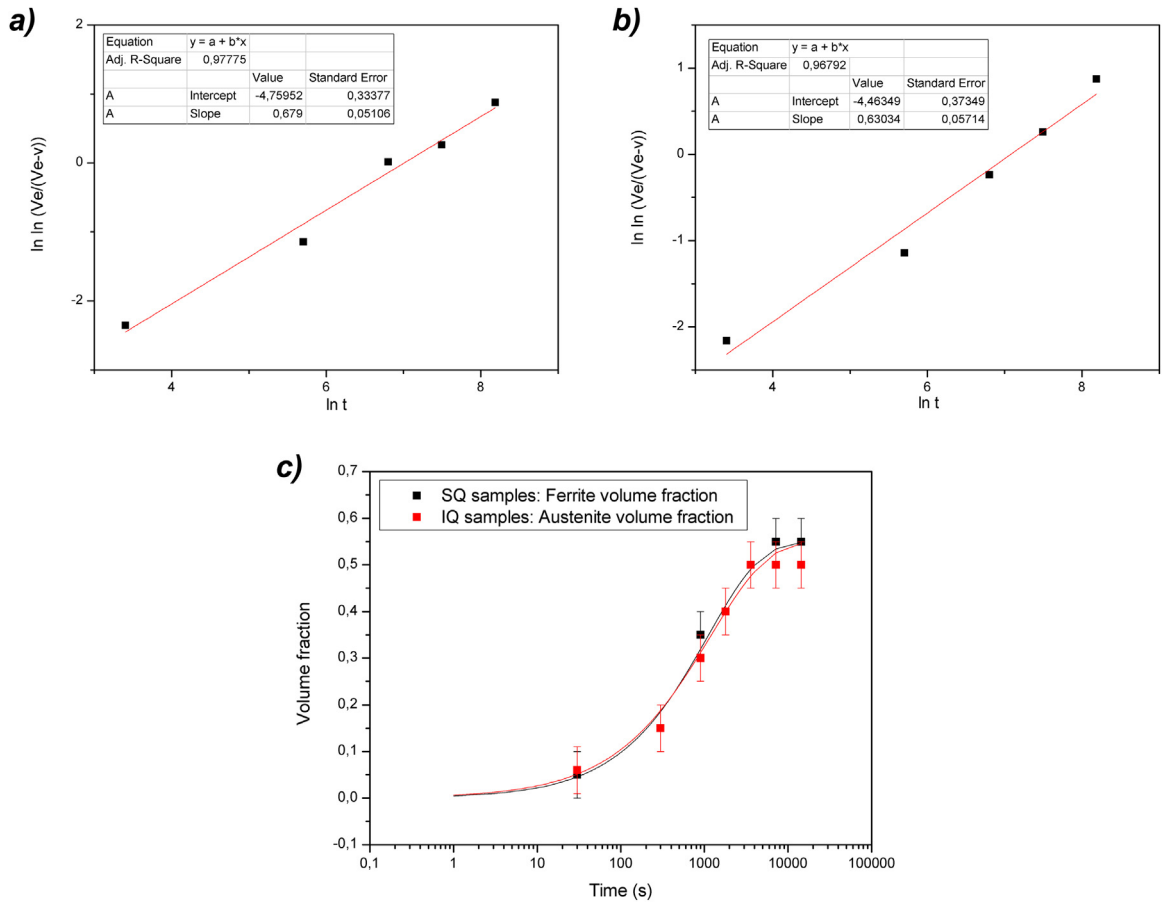

Fig. 10. $\ln\ln(\frac{V_e}{V_e - V_\alpha})$ vs $ln\, t$ at the intercritical temperature of 830 °C: (a) SQ samples, (b) IQ samples, (c) experimental data (points) and model prediction (solid line) for the kinetic of transformation at the intercritical temperature.

for a better determination of the Avrami´s exponent: one was held 30 s at the intercritical temperature and the rest 2 and 4 h at the same temperature. They were called SQ_0.5, SQ_120, SQ_240 and IQ_0.5, IQ_120, IQ_240. The sample SQ_240 and IQ_240, respectively, were used to determine the equilibrium volume fraction V_e.

The proportion of phases using the point counting method and the image J software were summarized in Table 2.

Now, the transformed volume fraction at any time can be determined as:

$$\frac{V_e - V_\alpha}{V_e} = \exp(-kt^n) \Rightarrow \ln\ln\left(\frac{V_e}{V_e - V_\alpha}\right) = \ln k + n \ln t \quad (3)$$

The plot of $\ln\ln(\frac{V_e}{V_e - V_\alpha})$ vs $ln\, t$ can be represented by a straight line, where the slope is the Avrami's exponent and the intersection with the vertical axis the constant k. This graph is observed in Fig. 10**a** for SQ samples and in Fig. 10**b** for IQ samples along with the linear approximation and Fig. 10**c** shows the Avrami's model (solid lines) and experimental data (scatter points) for both SQ and IQ samples.

Avrami's exponent n depends on the nature of nucleation and growth [25] and it can vary between 0.5 and 4 [26]. In the growth controlled by diffusion processes, n varies between 0.5 and 2.5 [27]. For SQ and IQ samples n = 0.68 and 0.63 respectively, which means that the kinetics of transformation for both groups of samples at 830 °C is a diffusion-controlled growth process.

5. Conclusions

The experimental results obtained and presented in this article allow to draw the following major conclusions:

1) A DP microstructure with similar tensile properties to that of the commercial DP steel was obtained by intermediate quenching (IQ) heat treatment. The step quenching heat treatment (SQ) seems not to be beneficial for commercial purpose, due mainly to the lack of suitable elongation.
2) The starting microstructure that precedes the intecritical temperature plays a decisive role on tensile properties.
3) Holding time and proportion of present phases seems not to be relevant in determining the tensile properties of the SQ or IQ samples.

Acknowledgements

This work was supported by Agencia Nacional de Promoción Científica y Tecnológica under grant number PICT-2014-0341 and Consejo Nacional de Investigaciones Científicas y Técnicas (CONICET) PIP-0426. The authors acknowledge Dr. Roberto Bruna TERNIUM SIDERAR for the donation of the DP.

Data availability

The raw and processed data required to reproduce these findings cannot be shared at this time as the data also forms part of an ongoing study.

References

[1] M.H. Saleh, R. Priestner, Retained austenite in dual-phase silicon steels and its effect on mechanical properties, J. Mater. Process. Technol. 113 (2001) 587–593.
[2] A. Bayram, A. Uguz, M. Ula, Effects of microstructure and notches on the mechanical properties of dual-phase steels, Mater. Charact. 43 (1999) 259–269.

[3] S. Curtze, V.-T. Kuokkalaa, M. Hokkaa, P. Peura, Deformation behavior of TRIP and DP steels in tension at different temperatures over a wide range of strain rates, Mater. Sci. Eng. A 507 (2009) 124–131.
[4] M.R. Akbarpour, A. Ekrami, Effect of ferrite volume fraction on work hardening behavior of high bainite dual phase (DP) steels, Mater. Sci. Eng. A 477 (2008) 306–310.
[5] A. Zare, A. Ekrami, Effect of martensite volume fraction on work hardening behavior of triple phase (TP) steels, Mater. Sci. Eng. A 528 (2011) 4422–4426.
[6] J. Zhang, H. Di, Y. Deng, R.D.K. Misra, Effect of martensite morphology and volume fraction on strain hardening and fracture behavior of martensite–ferrite dual phase steel, Mater. Sci. Eng. A 627 (2015) 230–240.
[7] N.J. Kim, G. Thomas, Effect of morphology on the mechanical behaviour of a dual-phase Fe/2Si/ 0.10C steel, Metall. Trans. A 12 (1981) 483–489.
[8] P.H. Chang, A.G. Preban, The effect of ferrite grain size and martensite volume fraction on the tensile properties of dual phase steel, Acta Metall. Mater. 33 (1985) 897–903.
[9] B.C. Hwang, T.Y. Cao, S.Y. Shin, S.H. Kim, S.H. Lee, S.J. Kim, Effects of ferrite grain size and martensite volume fraction on dynamic deformation behaviour of 0.15 C-2.0 Mn-0.2 Si dual phase steels, Mater. Sci. Technol. 21 (2005) 967–975.
[10] L.F. Ramos, D.K. Matlock, G. Krauss, On the deformation behavior of dual-phase steels, Metall. Trans. A 10 (1979) 259–261.
[11] N.K. Balliger, T. Gladman, Work hardening of dual-phase steels, Met. Sci. 15 (1981) 95–108.
[12] Alfirano, Samdan, Maulud, Effect of intercritical annealing temperature and holding time on microstructure and mechanical properties of dual phase low carbon steel, Appl. Mech. Mater. 493 (2014) 721–726.
[13] Havva K. Zeytin, Ceylan Kubilay, H.üseyin Aydin, Investigation of dual phase transformation of commercial low alloy steels: effect of holding time at low inter-critical annealing temperatures, Mater. Lett. 62 (2008) 2651–2653.
[14] K.W. Andrews, Empirical formulae for the calculation of some transformation temperatures, JISI 203 (1965) 721.
[15] E 562-02, Annual Book of ASTM Standards 03. 01 ASTM, Philadelphia, PA, 1993.
[16] E 8M, Annual Book of ASTM Standards 03. 01 ASTM, Philadelphia, PA, 1999.
[17] G. Krauss, Steels: Processing, Structure, and Performance, first ed., ASM International, 2005.
[18] N.J. Kim, A.H. Nakagawa, Effective grain size of dual-phase steel, Mater. Sci. Eng. A 83 (1986) 145–149.
[19] Y. Hu, X. Zuo, R. Li, Z. Zhang, Effect of initial microstructures on the properties of ferrite-martensite dual-phase pipeline steels with strain-based design, Mater. Res. 15 (2012) 317–322.
[20] M. Cacagnotto, Y. Adachi, D. Ponge, D. Raabe, Deformation and fracture mechanisms in fine- and ultrafine-grained ferrite/martensite dual-phase steels and the effect of aging, Acta Mater. 59 (2011) 658–670.
[21] S. Hashmi, Comprehensive Materials Finishing 1 Elsevier, 2017.
[22] F.C. Campbell, Phase Diagrams: Understanding the Basics, ASM International, Ohio, USA, 2012.
[23] Y. Liu, L. Zhang, Y. Du, D. Yu, D. Liang, Atomic mobility, uphill diffusion and pro-eutectic ferrite growth in Fe-Mn-C alloys, CALPHAD: Comput. Coupling Phase Diagr. Thermo-Chem. 33 (2009) 614–623.
[24] B.J. Kooi, Extension of the Johnson-Mehl-Avrami-Kolmogorov theory incorporating anisotropic growth studied by Monte Carlo simulations, Phys. Rev. B 73 (2006) 1–13.
[25] R.C. Sharma, Phase transformation in Materials, CBS, India, 2002, p. 146.
[26] J. Burk, Kinetics of Phase Transformation in Metals, Pergamon, London, 1965.
[27] E.S. Machlin, An Introduction to Aspects of Thermodynamics and Kinetics Relevant to Material Science, third ed., Elsevier, Amsterdam, 2007.